Sub-TeV H^+ Boson Production as Probe of Extra Top Yukawa Couplings

Dilip Kumar Ghosh,[1] Wei-Shu Hou,[2] and Tanmoy Modak[2]
[1]School of Physical Sciences, Indian Association for the Cultivation of Science, Kolkata 700032, India
[2]Department of Physics, National Taiwan University, Taipei 10617, Taiwan

(Received 30 December 2019; revised 9 July 2020; accepted 30 October 2020; published 24 November 2020)

We suggest searching for the charged Higgs boson at the Large Hadron Collider (LHC) via $cg \to bH^+ \to bt\bar{b}$. In the general two Higgs doublet model, extra top Yukawa couplings ρ_{tc} and ρ_{tt} can drive the disappearance of antimatter from the Universe, while $\bar{c}bH^+$ and $\bar{t}bH^+$ couple with strength $\rho_{tc}V_{tb}$ and $\rho_{tt}V_{tb}$, respectively. For $\rho_{tc}, \rho_{tt} \sim 0.5$, and $m_{H^+} \sim 300$–500 GeV, evidence could emerge from LHC run 2 data at hand and discovery by adding run 3 data in the near future.

DOI: 10.1103/PhysRevLett.125.221801

Introduction.—The discovery of the Higgs boson $h(125)$ at the LHC [1] suggests a weak scalar doublet, but there is no principle that precludes the existence of a second doublet. Having two Higgs doublets (2HDM), one has a charged H^+ boson plus the CP-even and -odd scalar bosons H, A [2]. We propose a novel process, $cg \to bH^+$ (see Fig. 1) followed by $H^+ \to t\bar{b}$, that may lead to the discovery of the exotic H^+ boson in the near future.

In the popular 2HDM type II (2HDM-II), up- and down-type quark masses arise from separate doublets [2], hence mass and Yukawa matrices are simultaneously diagonalized, just like in the standard model (SM). The model motivates an H^+ search at the LHC via the process $\bar{b}g \to \bar{t}H^+$ [3,4], which goes through the $\bar{t}bH^+$ coupling, while the $cg \to bH^+$ process is suppressed by the Cabibbo-Kobayashi-Maskawa (CKM) matrix element ratio $|V_{cb}/V_{tb}|^2 \sim 1.6 \times 10^{-3}$. But in the general 2HDM (g2HDM) with *extra* Yukawa couplings [5], $\bar{c}bH^+$ and $\bar{t}bH^+$ couple with strength $\rho_{tc}V_{tb}$ and $\rho_{tt}V_{tb}$, respectively, and $cg \to bH^+$ is not CKM suppressed.

The extra top Yukawa couplings [5] ρ_{tc} and ρ_{tt} are not well constrained. If both are $\mathcal{O}(1)$, i.e., the top Yukawa coupling strength λ_t in SM, they facilitate the production and decay in $cg \to bH^+ \to bt\bar{b}$ [6,7], with the signature of lepton plus missing energy and three b jets. It is known [8] that ρ_{tc} and ρ_{tt} at $\mathcal{O}(1)$ can *each* drive electroweak baryogenesis (EWBG) and hence account for the disappearance of antimatter shortly after the big bang, one of the biggest mysteries. Perhaps equally interesting, when the ACME 2018 bound [9] on electron electric dipole moment seemed to rule out the ρ_{tt} parameter space of Ref. [8], a second paper [10] brought in the extra electron Yukawa coupling ρ_{ee} and showed that a natural cancellation mechanism can survive the ACME18 bound and with expanded parameter space for EWBG. This gives strong motivation for the $cg \to bH^+ \to bt\bar{b}$ search. The recent CMS hint of an "excess" [11] in $gg \to A \to t\bar{t}$ at $m_A \sim 400$ GeV could also arise from $\rho_{tt} \sim \mathcal{O}(1)$ [12].

In this Letter, we first show that the H, A, and H^+ bosons in g2HDM can be sub-TeV in mass while satisfying all known constraints. This is in contrast with the absence of beyond SM signatures so far at the LHC, with bounds often reaching multi-TeV in scale. We then show that ρ_{tc}, ρ_{tt} at $\mathcal{O}(1)$ is allowed by current $\bar{b}g \to \bar{t}H^+$ and other search bounds. Full run 2 data could already give evidence for $cg \to bH^+ \to bt\bar{b}$, and discovery is possible by adding run 3 data.

Dimension-4 Higgs couplings.—In addition to gauge couplings, Higgs bosons uniquely possess two additional sets of dimension-4 couplings: Higgs quartic and Yukawa interactions. In the Higgs basis, one can write the most general CP-conserving potential [13,14] in g2HDM as

$$\begin{aligned} V(\Phi,\Phi') = {} & \mu_{11}^2|\Phi|^2 + \mu_{22}^2|\Phi'|^2 - (\mu_{12}^2\Phi^\dagger\Phi' + \text{H.c.}) \\ & + \frac{1}{2}\eta_1|\Phi|^4 + \frac{1}{2}\eta_2|\Phi'|^4 + \eta_3|\Phi|^2|\Phi'|^2 + \eta_4|\Phi^\dagger\Phi'|^2 \\ & + \left[\frac{1}{2}\eta_5(\Phi^\dagger\Phi')^2 + (\eta_6|\Phi|^2 + \eta_7|\Phi'|^2)\Phi^\dagger\Phi' + \text{H.c.}\right], \end{aligned} \tag{1}$$

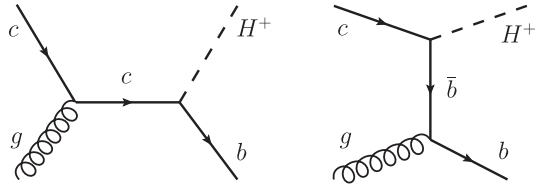

FIG. 1. Feynman diagrams for $cg \to bH^+$.

where all quartic couplings η_i are real, Φ induces spontaneous symmetry breaking by the vacuum expectation value v, i.e., $\mu_{11}^2 = -\frac{1}{2}\eta_1 v^2 < 0$, while $\langle \Phi' \rangle = 0$ hence $\mu_{22}^2 > 0$. The minimization condition $\mu_{12}^2 = \frac{1}{2}\eta_6 v^2$ reduces the parameter count to nine. From Eq. (1) one finds $m_{h^{(0)}}^2 = \eta_1 v^2$, $m_{H^\pm}^2 = \mu_{22}^2 + \frac{1}{2}\eta_3 v^2$, and $m_{H^{(0)},A}^2 = m_{H^+}^2 + \frac{1}{2}(\eta_4 \pm \eta_5)v^2$. Finally, η_6 mixes $h^{(0)}$ and $H^{(0)}$ into h and H. The emergent alignment phenomenon, that h resembles the Higgs boson of the SM so well [15–17], implies that the h–H mixing angle $c_\gamma \equiv \cos\gamma$ [denoted usually as $-\cos(\beta-\alpha)$] is rather small.

The Yukawa couplings to quarks are [13,14]

$$\begin{aligned}\mathcal{L} = -\frac{1}{\sqrt{2}}\sum_{f=u,d}\bar{f}_i[&(-\lambda_i^f\delta_{ij}s_\gamma + \rho_{ij}^f c_\gamma)h \\ &+ (\lambda_i^f\delta_{ij}c_\gamma + \rho_{ij}^f s_\gamma)H - i\mathrm{sgn}(Q_f)\rho_{ij}^f A]Rf_j \\ &- \bar{u}_i[(V\rho^d)_{ij}R - (\rho^{u\dagger}V)_{ij}L]d_j H^+ + \mathrm{H.c.},\end{aligned} \tag{2}$$

where $\lambda_i^f = \sqrt{2}m_i^f/v$, $L,R = (1 \mp \gamma_5)/2$, and $s_\gamma \equiv \sin\gamma$. Note that the A, H^+ couplings are independent of c_γ, while in the alignment limit of $c_\gamma \to 0$, h couples diagonally and H carries the extra Yukawa couplings ρ_{ij}^f. Thus, besides mass-mixing hierarchy protection [18–20] of flavor changing neutral Higgs couplings, alignment provides [14] further safeguard, without the need of natural flavor conservation [21]. The importance of ρ_{tt} and ρ_{tc} was emphasized [5] already at the $h(125)$ discovery and was subsequently shown [8] to possibly drive EWBG.

From Eq. (2) one finds that the leading $\bar{c}bH^+$ and $\bar{t}bH^+$ couplings are $\rho_{tc}V_{tb}$ and $\rho_{tt}V_{tb}$, respectively [22], where there is no CKM suppression of the former [24] as in 2HDM-II. In this Letter, we take $m_{H^+} > m_t$ [25] and focus on the $cg \to bH^+ \to bt\bar{b}$ process at the LHC. Note that the $gg \to \bar{c}bH^+$ process discussed in Ref. [7] bears some similarity, but Fig. 1 (left) was not mentioned explicitly, and a detailed collider study was not performed, hence the promise was not sufficiently demonstrated.

Constraints on Higgs parameters.—Higgs quartics need to satisfy positivity, perturbativity, and tree-level unitarity, which we implement via 2HDMC [26]. We express [13,14] η_1, η_{3-6} in terms of μ_{22}, m_{h,H,A,H^+} (all normalized to v), and $\cos\gamma$, plus η_2, η_7 that do not enter Higgs masses. Since H^+ Yukawa couplings do not depend on c_γ, which is known to be small, we set $c_\gamma = 0$ for simplicity while fixing $m_h \cong 125$ GeV, hence [14] $\eta_6 = 0$ and $\eta_1 = m_h^2/v^2$. Thus, e.g., $t \to ch$ does not constrain ρ_{tc}. In the common Higgs basis, we identify η_{1-7} with the input parameters Λ_{1-7} to 2HDMC.

For fixed m_{H^+}, we randomly generate the parameters in the ranges $|\eta_{2-5,7}| \le 3$ (positivity requires $\eta_2 > 0$), $\mu_{22} \in [0,1]$ TeV, and $m_{A,H} \in [m_{H^+} - m_W, 650\ \mathrm{GeV}]$ to forbid $H^+ \to AW^+, HW^+$. We then use 2HDMC for scanning, where the electroweak oblique parameter constraints (including correlations) are imposed, e.g., the 2σ range of $-0.17 < T < 0.35$ [27], which restricts [28,29] the scalar masses, hence the η_i's. Scan points satisfying these constraints are plotted in Fig. 2 in the m_H–m_A plane for $m_{H^+} = 300$ and 500 GeV, illustrating that finite parameter space exists. We choose a benchmark for each m_{H^+} value and list the parameters in Table I. More details of our scanning procedure is given in Ref. [30].

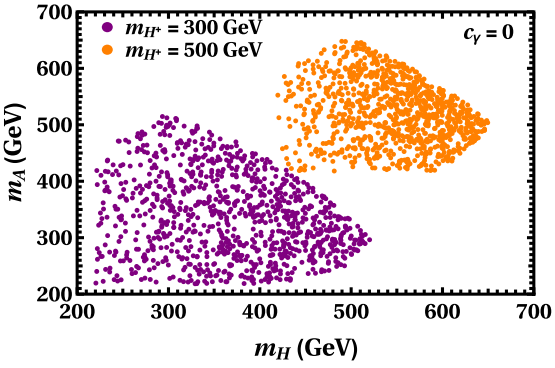

FIG. 2. Scan points in m_H–m_A plane that pass positivity, perturbativity, unitarity, and oblique parameter constraints.

Flavor constraints.—Flavor constraints on ρ_{tt} and ρ_{tc} are not particularly strong [5,31]. For $m_{H^+} \lesssim 500$ GeV, B_q mixings ($q = d,\ s$) provide the most stringent constraint. An H^+ effect from ρ_{ct} to the M_{12}^q amplitude is enhanced by $|V_{cq}/V_{tq}| \sim 25$, hence ρ_{ct} must be turned off [31]. Assuming all ρ_{ij} vanish except ρ_{tt}, we have $M_{12}^q/M_{12}^{q|\mathrm{SM}} = C_{B_q}$, with negligible phase. Allowing 2σ error on $C_{B_d} = 1.05 \pm 0.11$ and $C_{B_s} = 1.11 \pm 0.09$ [32], we find the blue shaded exclusion region (extending to upper right) in Fig. 3, where the left (right) panel is for BP1 (BP2). The constraint from H^+ effects via charm loops [33] gives $\rho_{tc} \lesssim 1(1.7)$ for BP1 (BP2).

$B \to X_s\gamma$ puts a strong constraint on m_{H^+} in 2HDM-II, but weakens for g2HDM due to extra Yukawa couplings. In fact, an m_t/m_b enhancement factor constrains ρ_{bb} more strongly [31] than ρ_{tt}. Taking ρ_{bb} as small, the constraint on ρ_{tt} falls outside the range of Fig. 3. The $B \to X_s\gamma$ constraint on ρ_{tc} via charm loop is weaker than B_q mixing [31]. Note that flavor constraints would grow weaker for m_{H^+} heavier than our benchmarks.

Collider constraints.—To focus on our signal process, we set all $\rho_{ij} = 0$ except ρ_{tt} and ρ_{tc} for simplicity.

For finite ρ_{tt}, one can have $\bar{b}g \to \bar{t}(b)H^+$ [34] followed by $H^+ \to t\bar{b}$ (charge conjugate process implied). Searches at 13 TeV provide model-independent bounds on

TABLE I. Benchmark points BP1 and BP2, with $\eta_6 = 0$, hence $\eta_1 \cong 0.258$. Higgs masses are in GeV.

	η_2	η_3	η_4	η_5	η_7	μ_{22}^2/v^2	m_{H^+}	m_A	m_H
BP1	1.40	0.62	0.53	1.06	−0.79	1.18	300	272	372
BP2	0.71	0.69	1.52	−0.93	0.24	3.78	500	569	517

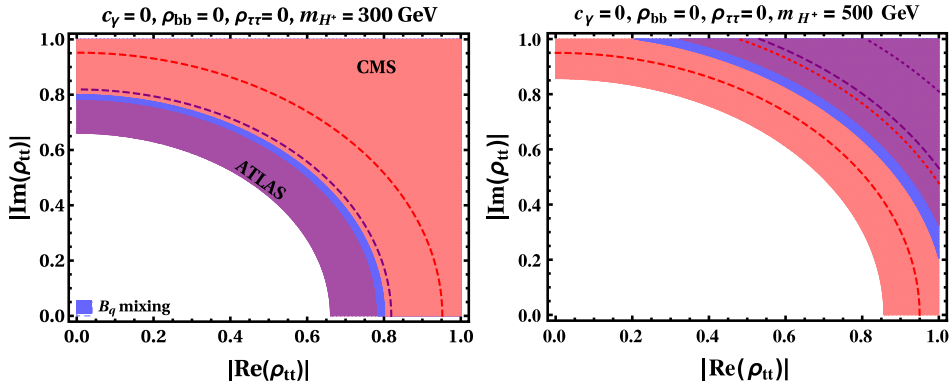

FIG. 3. Constraint from B_q mixings on ρ_{tt} (blue shaded region with area to upper right excluded) assuming all other $\rho_{ij} = 0$. The excluded regions from $bg \to \bar{t}(b)H^+ \to \bar{t}(b)t\bar{b}$ searches by ATLAS [3] and CMS [4] for $\rho_{tc} = 0$ are overlaid (purple and red shaded), which is weakened for $\rho_{tc} = 0.4$ (dash) and 0.8 (dots). See text for details.

$\sigma[pp \to \bar{t}(b)H^+]\mathcal{B}(H^+ \to t\bar{b})$, for $m_{H^+} = 200$ GeV to 2 (3) TeV for ATLAS [3] (CMS [4]). Using the Monte Carlo event generator (left)_aMC@NLO [35] with default NN23LO1 parton distribution function (PDF) [36] and effective model implemented in FeynRules2.0 [37], we calculate $\sigma[pp \to \bar{t}(b)H^+](H^+ \to t\bar{b})$ at leading order (LO) for a reference $|\rho_{tt}|$, then rescale by $|\rho_{tt}|^2\mathcal{B}(H^+ \to t\bar{b})$ to get the upper limits. For $m_{H^+} = 300$ and 500 GeV and with $\rho_{tc} = 0$ [hence $\mathcal{B}(H^+ \to t\bar{b}) \sim 100\%$], we plot the extracted ATLAS (CMS) 95% C.L. bounds on ρ_{tt} as the red (purple) shaded regions in Fig. 3. The ATLAS (CMS) limit is more (less) stringent than B_q mixing for BP1 ($m_{H^+} = 300$ GeV), while opposite for BP2 ($m_{H^+} = 500$ GeV). The exclusion bands are overlaid to illustrate this.

Heavy Higgs searches via $gg \to H/A \to t\bar{t}$ can constrain ρ_{tt}. ATLAS [38] searched at 8 TeV for $m_{A/H} > 500$ GeV; with 36 fb^{-1} at 13 TeV, CMS constrains the "coupling modifier" [11] for $m_{A/H} = 400$–750 GeV for various $\Gamma_{A/H}/m_{A/H}$ values. Both ranges are above BP1, while for BP2 the bounds are weaker than results shown in Fig. 3 (right). The CMS excess at $m_A \sim 400$ GeV [11] is discussed later.

Based on 137 fb^{-1} at 13 TeV, the CMS $4t$ search [39] constrains ρ_{tc} and ρ_{tt}. We first note that the direct limits from $\sigma(pp \to t\bar{t}A/t\bar{t}H)\mathcal{B}(A/H \to t\bar{t})$ for $m_{A/H} \in [350, 650]$ GeV are again weaker than results shown Fig. 3. With both ρ_{tc} and ρ_{tt} finite, the $cg \to tH/tA \to tt\bar{t}$ process [40] can feed the signal region, SR12, of the CMS $4t$ search if all three top quarks decay semileptonically. As $cg \to tH/tA \to tt\bar{t}$ barely occurs for BP1 because of low $m_{A,H}$ values, this applies only to BP2. SR12 requires [39] at least three leptons, four jets with at least three b tagged, plus missing p_T. Following Ref. [12], we generate events and interface with PYTHIA6.4 [41] for showering and hadronization, adopt MLM merging [42] of matrix element and parton shower, then feed into DELPHES3.4.2 [43] for CMS-based fast detector simulation, including b tagging and c- and light-jet rejection. We find $\rho_{tt} \gtrsim 1$ is excluded if $\rho_{tc} \sim 0.8$ for BP2. Noting that $H^+ \to c\bar{b}$ decay from finite ρ_{tc} would dilute $\mathcal{B}(H^+ \to t\bar{b})$ and soften the $bg \to \bar{t}(b)H^+$ constraint, we illustrate this effect by the dash (dot) curves in Fig. 3 (right) for $\rho_{tc} = 0.4(0.8)$.

The $cg \to tH/tA \to tt\bar{c}$ process [40] can feed the control region for $t\bar{t}W$ (CRW) background of CMS $4t$ study when both tops decay semileptonically. With CRW defined by same-sign dileptons (e or μ), p_T^{miss}, and up to five jets with at least two b tagged, we follow Refs. [12,44] and find $\rho_{tc} \gtrsim 0.4$ is excluded for BP1, which is stronger than the B_q mixing bound and with little dependence on ρ_{tt}. For BP2, we find that CRW gives comparable limit as SR12. Thus, we illustrate in Fig. 3 (left) the softened $bg \to \bar{t}(b)H^+$ constraint only for $\rho_{tc} = 0.4$.

We remark in passing that the ATLAS search for same-sign dileptons and b jets [45], or search for supersymmetry in similar event topologies [46], impose stronger cuts and, in general, do not give relevant constraints.

Collider signature for $cg \to bH^+ \to bt\bar{b}$.—We now show that the $cg \to bH^+ \to bt\bar{b}$ process, or $pp \to bH^+ + X \to bt\bar{b} + X$, is quite promising.

For illustration, we *conservatively* take $|\rho_{tc}| = 0.4$ and $|\rho_{tt}| = 0.6$ for both BPs. Receiving no CKM suppression, the approximate $H^+ \to c\bar{b}, t\bar{b}$ branching ratios are 50%, 50% for BP1, and 36%, 64% for BP2. Assuming $t \to b\ell\nu_\ell$ ($\ell = e, \mu$), the signature is one charged lepton p_T^{miss} and three b jets. Subdominant contributions such as PDF-suppressed $bg \to \bar{c}H^+, \bar{t}H^+ \to \bar{c}t\bar{b}, \bar{t}c\bar{b}$ with c jet mistagged as b jet, and ρ_{tt}-induced $bg \to \bar{t}H^+ \to \bar{t}t\bar{b}$ with one top decaying hadronically, are included as signal. There is also $c\bar{b} \to H^+ \to c\bar{b}, t\bar{b}$ [47], but these suffer from QCD and top backgrounds. The dominant backgrounds for $cg \to bH^+$ arise from $t\bar{t}$ + jets, t- and s-channel single-top (tj), Wt + jets, with subdominant backgrounds from $t\bar{t}h$ and $t\bar{t}Z$. Minor contributions from Drell-Yan (DY) and W + jets, $4t$, $t\bar{t}W$, and tWh are combined under "other."

TABLE II. Background and signal (Sig., for $\rho_{tc} = 0.4$, $\rho_{tt} = 0.6$) cross sections (in femtobarn) at 14 TeV after selection cuts.

	$t\bar{t}j$'s	tj	Wtj's	$t\bar{t}h$	$t\bar{t}Z$	Other	$B_{\rm tot}$	Sig.
BP1	1546	42	27	4.2	1.5	3.1	1627	11.4
BP2	1000	27	16	2.9	1.2	1.9	1049	9.3

Signal and background samples are generated at LO for 14 TeV as before by MADGRAPH, interfaced with PYTHIA and fed into DELPHES for fast detector simulation adopting default ATLAS-based detector card. The LO $t\bar{t}+$ jets background is normalized to next-to-next-leading order (NNLO) by a factor of 1.84 [48], and factors of 1.2 and 1.47 [49] for t- and s-channel single top. The LO $Wt+$ jets background is normalized to next-to-leading (NLO) order by a factor of 1.35 [50], whereas the subdominant $t\bar{t}h$ and $t\bar{t}Z$ receive factors of 1.27 [51] and 1.56 [52]. The DY + jets background is normalized to NNLO by a factor of 1.27 [53]. Finally, the $4t$ and $t\bar{t}W^-$ ($t\bar{t}W^+$) cross sections at LO are adjusted to NLO by factors of 2.04 [35] and 1.35 (1.27) [54]. The tWh and $W+$ jets backgrounds are kept at LO. Correction factors for other charge conjugate processes are assumed to be the same, and the signal cross sections are kept at LO.

Events are selected with one lepton, at least three jets with three b tagged, and $E_T^{\rm miss} > 35$ GeV. Jets are reconstructed by an anti-k_t algorithm using radius parameter $R = 0.6$. The lepton p_T should be > 30 GeV, with all three b jet $p_T > 20$ GeV and pseudorapidity ($|\eta|$) of lepton and b jets < 2.5. The ΔR separation between a b jet and the lepton, or any b-jet pair, should be > 0.4. The sum of the lepton and three leading b-jet transverse momenta H_T should be > 350 (400) GeV for BP1 (BP2). We have not optimized the selection cuts for H_T, p_T, $E_T^{\rm miss}$, etc. The total background cross section $B_{\rm tot}$ after selection cuts and its various components, together with the signal cross section (Sig.), are given in Table II.

We estimate the statistical significance from Table II with $\mathcal{Z} = \sqrt{2[(S+B)\ln(1+S/B) - S]}$ [55]. For 137, 300, and 600 fb^{-1}, the significance for $cg \to bH^+$ is at $\sim 3.3\sigma$, 4.9σ, and 6.9σ ($\sim 3.4\sigma$, 5.0σ, 7.1σ) for BP1 (BP2). Reanalyzing the signal and backgrounds for 13 TeV at 137 fb^{-1}, we find similar significance. Thus, full run 2 data could already show evidence, and combining ATLAS and CMS data is encouraged. Discovery is possible with combined run 2 and 3 data.

Discussion and summary.—A 3.5σ local (1.9σ global) excess at $m_A \approx 400$ GeV was reported by CMS [11] in $gg \to A \to t\bar{t}$ search. The excess can be explained [12] with sizable $\rho_{tt} \sim 1.1$, $\rho_{tc} \sim 0.9$ for $m_H \gtrsim 500$ GeV, and $m_{H^+} \gtrsim 530$ GeV. The bound on m_H is from the $cg \to tH \to tt\bar{t}$ process, while the slightly higher bound on m_{H^+} arises from combining B_q mixing and $\bar{b}g \to \bar{t}H^+$ constraints and the opening of $H^+ \to AW^+$ decay. Although not our benchmark, for $m_A = 400$ GeV, $m_H, m_{H^+} = 500$ and 530 GeV, and $\rho_{tt} \sim 1.1$ and $\rho_{tc} \sim 0.9$, we find that $cg \to bH^+$ could reach up to 11σ significance with full run 2 data. While exciting if the excess is confirmed, it could also become problematic for the g2HDM if $cg \to bH^+$ is not seen.

So far we have not considered the ρ_{tu} coupling, which can induce $ug \to bH^+ \to bt\bar{b}$, where the valence PDF means stronger constraint [56] from CRW and SR12 of Ref. [39], which weakens for larger ρ_{tt}. Taking $\rho_{tt} = 0.6$ and all other $\rho_{ij} = 0$, we find the CRW of Ref. [39] excludes $|\rho_{tu}| \gtrsim 0.1(0.2)$ for BP1 (BP2) at 95% C.L., with constraint from SR12 weaker. Taking $\rho_{tu} = 0.1$ (a rather large value in view of mass-mixing hierarchy protection) and $\rho_{tt} = 0.6$, we find $\sim 3.2\sigma$ (2.7σ) significance for BP1 (BP2) with full run 2 data. If ρ_{tu}-induced bH^+ production dominates, the valence PDF in pp collisions would imply an asymmetry with $\bar{b}H^-$, i.e., a charge asymmetry of $t\bar{b}b\bar{b}$ vs $\bar{t}bb\bar{b}$. The effects from $bg \to \bar{u}H^+ \to \bar{u}t\bar{b}$ and $\bar{t}H^+ \to \bar{t}u\bar{b}$ are negligible. Note that $B \to \mu\bar{\nu}$ decay probes [23] the $\rho_{tu}\rho_{\tau\mu}$ product at Belle II.

One may have same-sign top signature via $cg \to tA/tH \to tt\bar{c}$. Following the same analysis of Refs. [40,44], we find BP1 may have $\sim 3.5\sigma$ significance with full run 2 data, but below $\sim 1\sigma$ for BP2 due to dilution from $A/H \to t\bar{t}$ decay and falling parton luminosity.

Single-top studies may contain $cg \to bH^+$ events. For $\rho_{tc} = 0.4$ and $\rho_{tt} = 0.6$, we find the combined cross sections for $pp \to H^+[t\bar{b}]j$ and $H^+[c\bar{b}]t$ can contribute 15.2 (2.9) pb for BP1 (BP2), well within the 2σ error of current t-channel single-top [57,58] measurements. The situation is similar for run 1 with s-channel single top.

We have not included uncertainties from scale dependence and PDF [59,60], where the latter is sizable for processes initiated by heavy quarks. Using LO signal cross sections can also bring in some uncertainties, e.g., higher order corrections [50,61] to $\sigma(bg \to tH^+)$ may be 30%–40% for $m_{H^+} \sim 300$–500 GeV. A detailed study of such uncertainties is left for the future and is part of the reason why we adopt conservative ρ_{tc} and ρ_{tt} values.

Finally, our 300–500 GeV mass range is not just for its promise. Significance can still be high at higher masses for larger ρ_{tc} and ρ_{tt}, but the decoupling μ_{22}^2 would have to become larger [14] (as can be seen from $\mu_{22}^2/v^2 \simeq 3.78$ for BP2 in Table I), which would start to damp the EWBG motivation. But the $cg \to bH^+$ process can certainly be pursued for heavier m_{H^+} at higher luminosities.

In summary, extra top Yukawa couplings ρ_{tc} and ρ_{tt} enter $\bar{c}bH^+$ and $\bar{t}bH^+$ couplings without CKM suppression, leading to the $cg \to bH^+ \to bt\bar{b}$ signature of lepton plus missing energy and three b jets. For conservative $\rho_{tc}, \rho_{tt} \sim 0.5$, evidence could already emerge with full LHC run 2 data for $m_{H^+} = 300$–500 GeV, with discovery at 300 fb^{-1} and beyond, which would unequivocally point to physics beyond the standard model.

We thank Kai-Feng Chen for discussions, and the support from MOST 106-2112-M-002-015-MY3 and 108-2811-M-002-537, and NTU 108L104019.

Note added.—Recently, we noticed that the result for $pp \to \bar{t}bH^+ \to \bar{t}bt\bar{b}$ search by ATLAS has been updated with full run 2 dataset [62]. We have checked that the chosen ρ_{tt} values for the BPs are still allowed by current data.

[1] G. Aad *et al.* (ATLAS Collaboration), Phys. Lett. B **716**, 1 (2012); S. Chatrchyan *et al.* (CMS Collaboration), *ibid.* **716**, 30 (2012).

[2] See e. g., G. C. Branco, P. M. Ferreira, L. Lavoura, M. N. Rebelo, M. Sher, and J. P. Silva, Phys. Rep. **516**, 1 (2012).

[3] M. Aaboud *et al.* (ATLAS Collaboration), J. High Energy Phys. 11 (2018) 085.

[4] A. M. Sirunyan *et al.* (CMS Collaboration), J. High Energy Phys. 01 (2020) 096; Adding the new all-jet result, A. M. Sirunyan *et al.* (CMS Collaboration), J. High Energy Phys. 07 (2020) 126; does not change our conclusions (the limit improves at second decimal place for $m_{H^+} = 300$ GeV, but makes no impact for 500 GeV).

[5] K.-F. Chen, W.-S. Hou, C. Kao, and M. Kohda, Phys. Lett. B **725**, 378 (2013).

[6] The process is mentioned without collider study in S. Iguro and K. Tobe, Nucl. Phys. **B925**, 560 (2017); We note also the paper by U. Nierste, M. Tabet, and R. Ziegler, Phys. Rev. Lett. **125**, 031801 (2020), posted after our work. See also Ref. [7] below and discussion in text.

[7] S. Gori, C. Grojean, A. Juste, and A. Paul, J. High Energy Phys. 01 (2018) 108.

[8] K. Fuyuto, W.-S. Hou, and E. Senaha, Phys. Lett. B **776**, 402 (2018).

[9] V. Andreev *et al.* (ACME Collaboration), Nature (London) **562**, 355 (2018).

[10] K. Fuyuto, W.-S. Hou, and E. Senaha, Phys. Rev. D **101**, 011901(R) (2020).

[11] A. M. Sirunyan *et al.* (CMS Collaboration), J. High Energy Phys. 04 (2020) 171.

[12] W.-S. Hou, M. Kohda, and T. Modak, Phys. Lett. B **798**, 134953 (2019).

[13] See, e.g., S. Davidson and H. E. Haber, Phys. Rev. D **72**, 035004 (2005).

[14] W.-S. Hou and M. Kikuchi, Europhys. Lett. **123**, 11001 (2018).

[15] G. Aad *et al.* (ATLAS and CMS Collaborations), J. High Energy Phys. 08 (2016) 045.

[16] A. M. Sirunyan *et al.* (CMS Collaboration), Eur. Phys. J. C **79**, 421 (2019).

[17] G. Aad *et al.* (ATLAS Collaboration), Phys. Rev. D **101**, 012002 (2020).

[18] W.-S. Hou, Phys. Lett. B **296**, 179 (1992).

[19] D. Chang, W.-S. Hou, and W.-Y. Keung, Phys. Rev. D **48**, 217 (1993).

[20] D. Atwood, L. Reina, and A. Soni, Phys. Rev. D **55**, 3156 (1997).

[21] S. L. Glashow and S. Weinberg, Phys. Rev. D **15**, 1958 (1977).

[22] Down-type contributions via $V_{cs}\rho_{sb}$ and $V_{tb}\rho_{bb}$ are suppressed by small ρ_{sb} due to B_s mixing constraint, while ρ_{bb} is expected to be far smaller than ρ_{tt} by mass-mixing hierarchy arguments; see, e.g., Ref. [23] for a recent discussion.

[23] W.-S. Hou, M. Kohda, T. Modak, and G.-G. Wong, Phys. Lett. B **800**, 135105 (2020).

[24] For a partial list of work on such $\bar{c}bH^+$ couplings, see, e.g., H.-J. He and C.-P. Yuan, Phys. Rev. Lett. **83**, 28 (1999); J. L. Diaz-Cruz, J. Hernández-Sánchez, S. Moretti, R. Noriega-Papaqui, and A. Rosado, Phys. Rev. D **79**, 095025 (2009); J. Hernandez-Sanchez, S. Moretti, R. Noriega-Papaqui, and A. Rosado, J. High Energy Phys. 07 (2013) 044; O. Flores-Sanchez, J. Hernández-Sánchez, C. G. Honorato, S. Moretti, and S. Rosado-Navarro, Phys. Rev. D **99**, 095009 (2019); J. Hernandez-Sanchez, C. G. Honorato, S. Moretti, and S. Rosado-Navarro, Phys. Rev. D **102**, 055008 (2020).

[25] This evades, e.g., the CMS search for $t \to bH^+$, $H^+ \to c\bar{b}$ for $m_{H^+} < 150$ GeV, A. M. Sirunyan *et al.* (CMS Collaboration), J. High Energy Phys. 11 (2018) 115.

[26] D. Eriksson, J. Rathsman, and O. Stål, Comput. Phys. Commun. **181**, 189 (2010).

[27] Taken from http://project-gfitter.web.cern.ch/project-gfitter/Oblique_Parameters/.

[28] C. D. Froggatt, R. G. Moorhouse, and I. G. Knowles, Phys. Rev. D **45**, 2471 (1992).

[29] H. E. Haber and O. Stål, Eur. Phys. J. C **75**, 491 (2015).

[30] W.-S. Hou, M. Kohda, and T. Modak, Phys. Rev. D **99**, 055046 (2019).

[31] B. Altunkaynak, W.-S. Hou, C. Kao, M. Kohda, and B. McCoy, Phys. Lett. B **751**, 135 (2015).

[32] http://www.utfit.org/UTfit/ResultsSummer2018NP.

[33] A. Crivellin, C. Greub, and A. Kokulu, Phys. Rev. D **87**, 094031 (2013).

[34] For a nonexhaustive list, see J. F. Gunion, H. E. Haber, F. E. Paige, W.-K. Tung, and S. S. D. Willenbrock, Nucl. Phys. **B294**, 621 (1987); J. L. Diaz-Cruz and O. A. Sampayo, Phys. Rev. D **50**, 6820 (1994); S. Moretti and D. P. Roy, Phys. Lett. B **470**, 209 (1999); D. J. Miller, S. Moretti, D. P. Roy, and W. J. Stirling, Phys. Rev. D **61**, 055011 (2000); A. Arhrib *et al.*, arXiv:1905.02635; J.-Y. Cen, J.-H. Chen, X.-G. He, G. Li, J.-Y. Su, and W. Wang, J. High Energy Phys. 01 (2019) 148; P. Sanyal, Eur. Phys. J. C **79**, 913 (2019); B. Coleppa, A. Sarkar, and S. K. Rai, Phys. Rev. D **101**, 055030 (2020).

[35] J. Alwall, R. Frederix, S. Frixione, V. Hirschi, F. Maltoni, O. Mattelaer, H.-S. Shao, T. Stelzer, P. Torrielli, and M. Zaro, J. High Energy Phys. 07 (2014) 079.

[36] R. D. Ball *et al.* (NNPDF Collaboration), Nucl. Phys. **B877**, 290 (2013).

[37] A. Alloul, N. D. Christensen, C. Degrande, C. Duhr, and B. Fuks, Comput. Phys. Commun. **185**, 2250 (2014).

[38] M. Aaboud *et al.* (ATLAS Collaboration), Phys. Rev. Lett. **119**, 191803 (2017).

[39] A. M. Sirunyan *et al.* (CMS Collaboration), Eur. Phys. J. C **80**, 75 (2020).

[40] M. Kohda, T. Modak, and W.-S. Hou, Phys. Lett. B **776**, 379 (2018).

[41] T. Sjöstrand, S. Mrenna, and P. Skands, J. High Energy Phys. 05 (2006) 026.
[42] M. L. Mangano, M. Moretti, F. Piccinini, and M. Treccani, J. High Energy Phys. 01 (2007) 013.
[43] J. de Favereau, C. Delaere, P. Demin, A. Giammanco, V. Lemaître, A. Mertens, and M. Selvaggi (DELPHES 3 Collaboration), J. High Energy Phys. 02 (2014) 057.
[44] W.-S. Hou, M. Kohda, and T. Modak, Phys. Lett. B **786**, 212 (2018).
[45] M. Aaboud *et al.* (ATLAS Collaboration), J. High Energy Phys. 12 (2018) 039.
[46] G. Aad *et al.* (ATLAS Collaboration), J. High Energy Phys. 06 (2020) 046.
[47] The inclusive $pp \to H^+$ cross section (up to two additional jets) in the five flavor scheme for BP1 (BP2) at 14 TeV is 50.8 (6.5) pb evaluated by MADGRAPH5_aMC with NN23LO1 PDF set and default run card.
[48] https://twiki.cern.ch/twiki/bin/view/LHCPhysics/TtbarNNLO.
[49] https://twiki.cern.ch/twiki/bin/view/LHCPhysics/SingleTopRefXsec.
[50] N. Kidonakis, Phys. Rev. D **82**, 054018 (2010).
[51] https://twiki.cern.ch/twiki/bin/view/LHCPhysics/CERNYellowReportPageAt14TeV2010.
[52] J. Campbell, R. K. Ellis, and R. Röntsch, Phys. Rev. D **87**, 114006 (2013).
[53] Y. Li and F. Petriello, Phys. Rev. D **86**, 094034 (2012).
[54] J. M. Campbell and R. K. Ellis, J. High Energy Phys. 07 (2012) 052.
[55] G. Cowan, K. Cranmer, E. Gross, and O. Vitells, Eur. Phys. J. C **71**, 1554 (2011).
[56] For more discussion on constraining ρ_{tu}, see W.-S. Hou, T.-H. Hsu, and T. Modak, Phys. Rev. D **102**, 055006 (2020).
[57] M. Aaboud *et al.* (ATLAS Collaboration), J. High Energy Phys. 04 (2017) 086.
[58] A. M. Sirunyan *et al.* (CMS Collaboration), Phys. Lett. B **800**, 135042 (2020).
[59] M. Buza, Y. Matiounine, J. Smith, and W. L. van Neerven, Eur. Phys. J. C **1**, 301 (1998).
[60] F. Maltoni, G. Ridolfi, and M. Ubiali, J. High Energy Phys. 07 (2012) 022.
[61] T. Plehn, Phys. Rev. D **67**, 014018 (2003); E. L. Berger, T. Han, J. Jiang, and T. Plehn, *ibid.* **71**, 115012 (2005).
[62] The ATLAS Collaboration, Report No. ATLAS-CONF-2020-039.